FMDB *Transactions on Sustainable Applied Sciences*

Noise Suppression in PMSM Drive System Using Random Pulse Position Modulation

Saravanan Sivasamy[1,*], K. N. Srinivas[2], Dinka Lale[3], Baltaeva Umida Ismoilovna[4], M. Shagar Banu[5]

[1,2]Department of Electrical and Electronics Engineering, SRM Institute of Science and Technology, Ramapuram, Chennai, Tamil Nadu, India.
[3]Faculty of Electrical Engineering and Applied Computing, University of Dubrovnik, Dubrovnik, Croatia.
[4]Department of Applied Mathematics and Mathematical Physics, Urgench State University, Urgench City, Khorezm Region, Uzbekistan.
[5]Department of Electrical and Electronics Engineering, Dhaanish Ahmed College of Engineering, Chennai, Tamil Nadu, India.
saravans13@srmist.edu.in[1], srinivak@srmist.edu.in[2], lariat@unidu.hr[3], umida_baltayeva@mail.ru[4], shagarbanu.m@dhaanishcollege.in[5]

Abstract: Permanent Magnet Synchronous Motor (PMSM) drives are widely utilised in robotics and industrial automation applications due to their superior efficiency, reliability, and dynamic performance. However, when powered via converter systems such as Indirect Matrix Converters (IMCs), these drives often experience significant high-frequency harmonic distortion due to conventional Space Vector Pulse Width Modulation (SVPWM) techniques. These harmonics adversely affect system performance by increasing electromagnetic interference (EMI), acoustic noise, and overall power losses, thereby degrading efficiency and electromagnetic compatibility (EMC). To address these issues, this paper proposes a Markov Chain Pseudorandom Asymmetrical Space Vector Modulation (MC-PRASVM) technique for high-frequency harmonic suppression in PMSM drives. The proposed method employs the stochastic behaviour of Markov chains to generate pseudorandom, asymmetric switching sequences. This dynamic switching approach effectively spreads harmonic energy across a broader frequency spectrum, thereby minimising harmonic concentration and resonance. Simulation and experimental analyses demonstrate that the MC-PRASVM technique significantly improves current waveform quality, reduces total harmonic distortion (THD), and enhances electromagnetic compatibility compared to traditional SVPWM strategies.

Keywords: Harmonic Suppression; Electromagnetic Interference (EMI); Space Vector; Robotic Applications; Electromagnetic Compatibility; Asymmetric Switching; Total Harmonic Distortion (THD).

Received on: 14/05/2024, **Revised on:** 01/08/2024, **Accepted on:** 14/11/2024, **Published on:** 03/06/2025

Journal Homepage: https://www.fmdbpub.com/user/journals/details/FTSASS

DOI: https://doi.org/10.69888/FTSASS.2025.000531

Cite as: S. Sivasamy, K. N. Srinivas, D. Lale, B. U. Ismoilovna, and M. S. Banu, "Noise Suppression in PMSM Drive System Using Random Pulse Position Modulation," *FMDB Transactions on Sustainable Applied Sciences*, vol. 2, no. 1, pp. 34–47, 2025.

1. Introduction

[*]Corresponding author.

Permanent Magnet Synchronous Motors (PMSMs) have gained widespread adoption across various industrial and commercial applications due to their high efficiency, excellent torque-to-weight ratio, and superior dynamic performance [1]. They are extensively used in electric vehicles, robotics, aerospace systems, CNC machines, and renewable energy systems such as wind turbines. In many of these applications, the motor drive system demands high precision, minimal noise, and higher power quality [2]. To meet these requirements, PMSMs are often powered by advanced converter topologies, such as the Indirect Matrix Converter (IMC), which offers benefits including bidirectional power flow, a compact structure, and the elimination of bulky DC-link capacitors [3]. In the IMC, the inverter stage commonly employs Space Vector Pulse Width Modulation (SVPWM) to generate output voltage waveforms. However, a major drawback of conventional SVPWM is the generation of high-frequency harmonics in the output current, particularly at integral multiples of the switching (carrier) frequency [4]. These harmonics contribute to electromagnetic interference (EMI), increased acoustic noise, heating losses, and reduced motor lifespan, all of which degrade overall system performance [5]. To address this, various Random Pulse Width Modulation (RPWM) techniques have been explored for harmonic suppression. While effective to some extent, conventional RPWM schemes have inherent limitations, such as spectral spreading without consistent attenuation of specific harmonic components [6]. In this context, a Markov Chain-based Random Asymmetrical Space Vector PWM (MRA-SVPWM) method is proposed to enhance harmonic suppression in IMC-fed PMSM drives. This technique leverages the memoryless property of Markov chains to generate non-repetitive stochastic switching sequences [7]. By dynamically altering the vector order and switching state according to Markov transition probabilities, MRA-SVPWM redistributes and reduces the concentration of harmonic energy within specific frequency bands [8].

PMSMs play a critical role in high-performance drive applications, including automotive systems, industrial automation, and renewable energy, thanks to their exceptional efficiency and power density [9]. Despite their advantages, conventional modulation techniques struggle with high-frequency harmonic distortion, resulting in undesirable torque ripple, increased acoustic noise, and excessive power losses—all of which negatively impact system efficiency and reliability [10]. Among various modulation techniques, SVPWM stands out as a widely adopted approach for PMSM inverter control, delivering enhanced voltage utilisation and lower harmonic distortion than traditional sinusoidal PWM methods [11]. However, even with its benefits, standard SVPWM techniques fall short of effectively mitigating high-frequency harmonics, particularly under varying load conditions [12]. Several random PWM (RPWM) strategies have been investigated as potential solutions, yet they often introduce challenges, such as unstable voltage regulation and increased computational complexity [13]. To overcome these limitations, this paper proposes an innovative Markov Chain Random Asymmetrical SVPWM (MRA-SVPWM) approach that leverages Markov-process-based stochastic switching sequences to achieve optimal harmonic suppression. Unlike conventional RPWM techniques, which rely solely on random switching variations, the MRA-SVPWM method introduces a structured randomness that significantly reduces dominant harmonics while preserving inverter voltage stability [14]. Extensive simulations and experimental evaluations confirm that MRA-SVPWM delivers superior harmonic suppression and lower acoustic noise, establishing it as a promising solution for next-generation PMSM drive applications. The following sections of this paper provide a foundation, implementation, and performance analysis of the SVPWM method, emphasising its key advantages over conventional techniques [15].

2. Modulation Strategy

An Indirect Matrix Converter (IMC) is a two-stage AC-AC power converter that directly converts a three-phase AC input to an AC output without energy storage components, such as DC-link capacitors. The IMC comprises three key components: an inverter stage. The LC filter is placed at the input to suppress high-frequency switching noise and improve power quality. The current drawn from the AC source is smooth and sinusoidal. The rectifier stage converts the filtered AC voltage into a virtual DC link—this is not a physically stored voltage like in traditional converters, but rather a continuously modulated voltage derived from controlled switching. The inverter stage then synthesises a new three-phase AC output from this virtual DC link, tailored to the load's voltage and frequency requirements—commonly a Permanent Magnet Synchronous Motor (PMSM) in modern industrial and automotive applications. To control both the rectifier and inverter stages, the IMC employs Space Vector Pulse Width Modulation (SVPWM). This advanced modulation technique enables precise, efficient control of switching devices (such as IGBTs and MOSFETs). SVPWM represents the desired output voltage as a rotating vector in a two-dimensional space (called the d-q or α-β plane).

This reference vector is then approximated by switching between adjacent voltage vectors for specific time intervals during each switching cycle. The switching patterns are determined by calculating duty ratios for the active vectors and, in the case of the inverter stage, also for the zero vectors, which do not contribute voltage but allow switching transitions. In the rectifier stage, only active current vectors are used, meaning the converter continuously draws current from the input. In contrast, the inverter stage uses both active and zero-voltage vectors to better shape the output waveform. The mathematical expressions for the duty ratios of the active vectors are derived using the modulation index and the angular position of the reference vector. For example, the duty ratios for the rectifier vectors (di1, di2) and inverter vectors (dv1, dv2) are functions of the angles θi and θv, respectively. The duty ratios of the inverter zero vectors (d0, d7) are calculated to occupy the remaining time in the switching

cycle not used by the active vectors. An important feature of IMC operation is the implementation of zero current commutation, which ensures that switching transitions in the rectifier stage occur safely without causing current surges or voltage spikes (Figure 1).

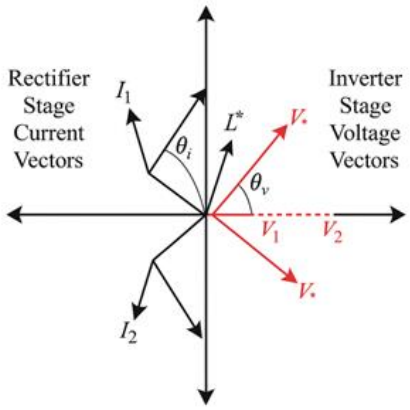

Figure 1: Vector diagram for SVPWM

This is achieved by aligning the rectifier commutation with the inverter's zero-vector intervals. During these intervals, the inverter does not supply any voltage to the output, and consequently, no current flows through the virtual DC link. This creates a safe window during which the rectifier switches can change state without current flow, minimising stress on the power devices and preventing shoot-through faults. By synchronising the rectifier and inverter switching strategies, the IMC achieves smooth transitions, lower switching losses, and improved overall efficiency (Figure 2).

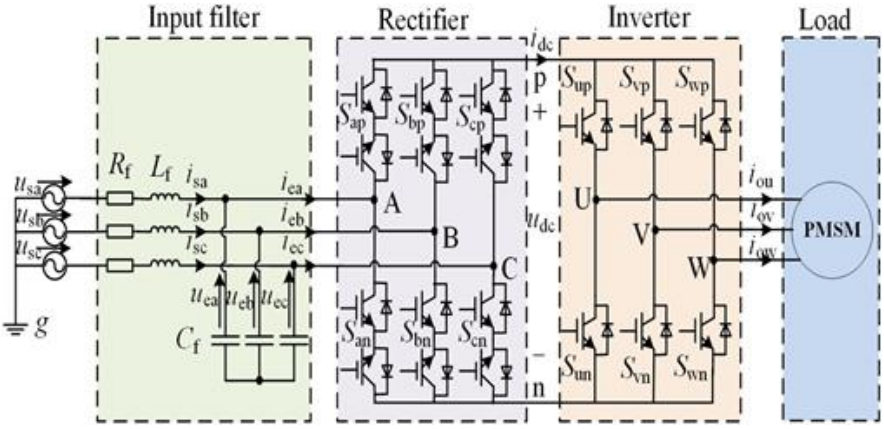

Figure 2: IMC-PMSM topology

3. Analytical Study of High-Frequency Harmonic Components in SVPWM

In Modulation (SVPWM), high-frequency harmonics primarily arise from the inverter's rapid switching. These harmonics are an unavoidable consequence of converting DC to AC using high-speed switches. The behaviour and structure of these harmonics can be analysed using time-varying mathematical functions. These functions are based on several variables, such as the frequencies and the grid, along with their initial phase angles. Harmonic components in SVPWM can generally be divided into four main categories: a constant DC component, low-frequency baseband components related to the grid or fundamental wave, mixed-frequency components caused by the interaction between the carrier and fundamental signals, and, finally, high-frequency components that cluster around multiples of the carrier frequency. These high-frequency harmonics typically appear at frequency points. Here k, m, n k, m, k, m, n are integers representing harmonic orders. For instance, when m = 1 and n = 2, researchers observe a second-order sideband harmonic near the first carrier frequency. In practical applications, engineers focus on harmonics near the first and second multiples of the carrier frequency, as they can significantly affect power quality. Using a three-dimensional Fourier transform, the amplitude of these harmonics can be mathematically calculated. Additionally, the SVPWM waveform itself contains primarily fundamental and third-harmonic components due to its structure. Higher-order harmonics exist but are often small in magnitude. To maximise the DC link voltage and minimise unwanted harmonics,

SVPWM divides the reference vector into sectors and adjusts the switching patterns accordingly. In each sector, one phase remains constantly on while the others are modulated. The result is efficient voltage use, but it also creates predictable harmonic patterns. These patterns depend strongly on carrier frequency, modulation index, and sector selection. Therefore, harmonic suppression can be achieved by adjusting modulation equation coefficients or by adopting alternative control strategies, such as random PWM or variable switching frequency (Figure 3).

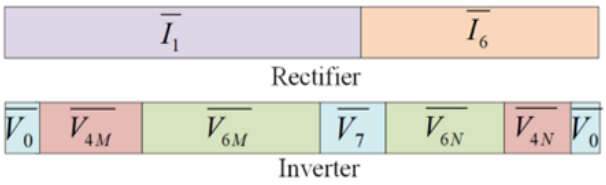

Figure 3: Vector distribution

4. Pulse Width Modulation

The Markov (RPWM) method is implemented to enhance the performance of variable-frequency speed control systems by improving the quality and distribution of random numbers used to determine switching frequencies. Conventionally, random switching frequency fs is derived from a base frequency f0, a random gain Δf, and a random number R, following the formula. fs=f0±Δf·R. Random numbers are typically generated using the linear congruence method, where each new number is determined by the previous one using the equation Rn+1=mod2N(Rn×P1+P2), with constants P1=29, P2=37, Ns=16. These values ensure a full-period cycle of the generator on a 16-bit microprocessor, covering the full range from 0 to 2^16, with the requirement that P1 is of the form 4K+1 and P2 is coprime to 2^N. However, conventional random number generation shows bias, with successive numbers tending to cluster on one side of the mean, reducing the effectiveness of harmonic dispersion in the frequency spectrum. To counter this, a two-state Markov chain is introduced into the RSFPWM system. Markov processes are memoryless, meaning the future state depends only on the present state, not on the past. This is modelled using a transition probability matrix Pij=P{Xn=j|Xm=i} where i, ji, and j are the states and Pij is the probability of transitioning from state I to j. In this RPWM application, the two states are defined as: 1) switching frequency less than the expected value, and 2) greater than the expected value. Two sets of random numbers, r1r_1r1 and r2r_2r2, are generated using different prime numbers (e.g., P1=97P_1 = 97P1=97, P2=59P_2 = 59P2=59 for r2r_2r2), where r1r_1r1 determines state transition and r2r_2r2 provides the actual switching frequency (Figure 4).

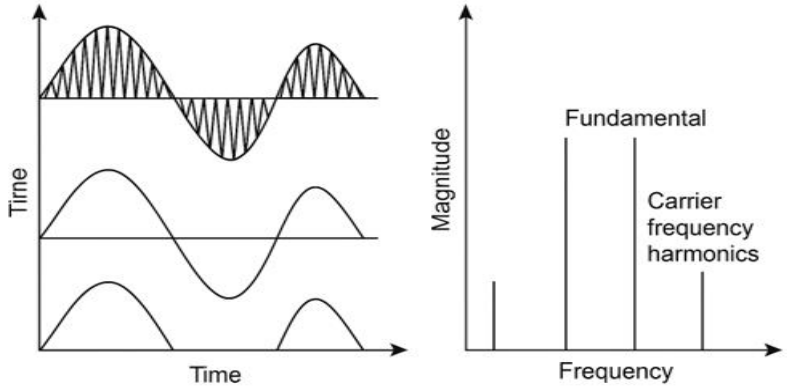

Figure 4: Effect of SVPWM on frequency

The best performance is observed at a transition probability Pt=0.8, which guides the switching behaviour between the two random sequences. The effectiveness of this approach is validated through multiple evaluations. Graphs of random number distributions and histograms show that Markov chain-generated numbers avoid clustering near the mathematical expectation (0.5), unlike conventional methods, leading to broader, more uniform harmonic dispersion in the frequency spectrum. Statistical measures such as the mean and standard deviation support this: the mean for conventional numbers is 0.526. In contrast, for Markov-based numbers, it is 0.507, much closer to the theoretical mean of 0.5. The deviation (D') for Markov numbers is higher (0.262) compared to conventional ones (0.215), indicating a wider spread in the number distribution, which is favourable for reducing harmonic peaks. Moreover, significance tests using the Kolmogorov–Smirnov method indicate that conventional random numbers approximate a normal distribution (p-value 0.169 > 0.05). In contrast, Markov-generated ones do not (p-value 0.011 < 0.05), suggesting a more random and unpredictable nature. Both types, however, conform to a uniform distribution

rather than a Poisson distribution. P–P plots further show that Markov chain random numbers deviate more from the theoretical normal distribution diagonal, reinforcing the claim of improved randomness. In conclusion, Markov chain-based RPWM provides superior random number quality, enhancing harmonic dispersion by avoiding clustering around integer multiples of switching frequency. This not only improves spectral performance but also reduces EMI and improves system stability in motor drives.

5. Asymmetrical SVPWM

Asymmetrical (SVPWM) is an advanced modulation strategy aimed at improving the harmonic performance of conventional SVPWM. It achieves this by increasing the equivalent switching frequency without increasing the carrier frequency, thereby enhancing harmonic suppression. Unlike conventional SVPWM, which employs a symmetric order of active vectors around the zero, asymmetrical SVPWM modifies the switching vector order in the latter half of the carrier cycle. For instance, in the first sector, conventional SVPWM follows the switching order: V (000) →V4(100) →V6(110) →V7(111) →V7(111) →V6(110) →V4(100) →V0(000). In contrast, asymmetrical SVPWM alters the second half of the sequence to: V0(000) →V4(100) →V6 (110) →V7(111) →V7(111) →V4(100) →V6(110) →V0(000). V (111) →V7(111) →V4 (100) →V6(110) →V0(000), thereby creating an asymmetry. This change leads to different switching behaviour in the inverter bridge arms: the intermediate-phase bridge arm switches four times per cycle, while the other two arms switch twice per cycle. Consequently, the total number of switching operations increases from 6 in conventional SVPWM to 8 in asymmetrical SVPWM, resulting in a 33% increase in the effective switching frequency. This increase improves harmonic attenuation in the output waveform. Additionally, when implemented in a two-stage system such as a rectifier-inverter configuration, asymmetrical SVPWM can be coordinated with the rectifier's switching states, thereby optimising overall system performance. By strategically altering the switching sequence sector-wise, this method not only minimises harmonics but also improves overall performance (Figure 5).

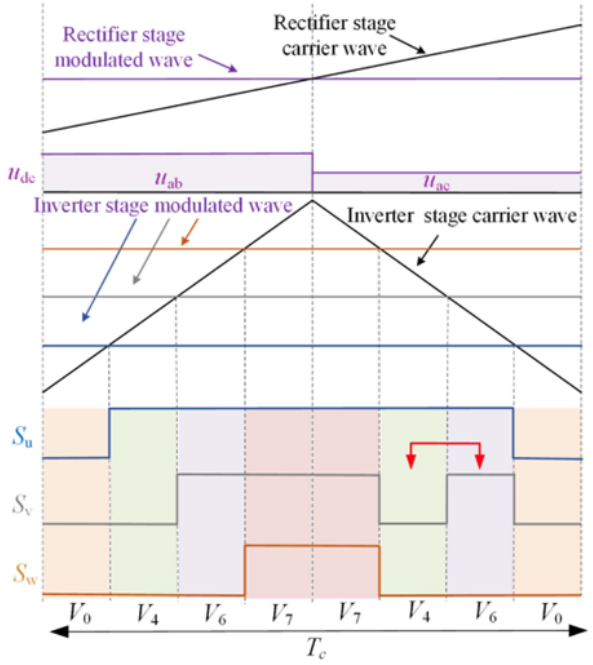

Figure 5: Diagram of asymmetrical SVPWM

6. Pseudo Random Asymmetrical

Markov Chain Random Asymmetrical Space Vector PWM (MRA-SVPWM) is a hybrid modulation strategy that integrates Markov Chain-based RPWM with Asymmetrical SVPWM to enhance inverter performance. This method is particularly effective at reducing harmonic distortion and achieving synchronised control of both the rectifier and the inverter stages. The Markov Chain RPWM component works by varying the carrier frequency in a controlled pseudorandom manner. These pseudorandom values, introduced earlier in the system, generate a variable-frequency carrier signal, which is then used to modulate three-phase PWM waveforms by altering the carrier frequency from cycle to cycle. The harmonic energy that would otherwise concentrate around multiples of a fixed carrier frequency is dispersed more evenly across the spectrum. This spreads the harmonics, effectively lowering peak distortion. In parallel, the Asymmetrical SVPWM portion enhances performance by

adjusting the active space vectors during each switching cycle. Unlike conventional SVPWM, which maintains a symmetric vector pattern around the zero vector, the asymmetrical variant reorders switching to increase the number of transitions, thus raising the equivalent switching frequency by around 33%. Importantly, these two techniques—Markov-based carrier modulation and asymmetrical signal modulation—operate independently and do not interfere with one another. They are functionally decoupled but synergistically contribute to harmonic suppression and better waveform quality. To evaluate the effects of this approach, three methods were compared: the standard in a system with a fixed carrier frequency of 6 kHz and the standard SVPWM results. When using the Markov Chain RPWM, the carrier frequency fluctuates between 4.8 and 7.2 kHz due to the pseudorandom variation, and the switching frequency directly follows this range. However, with MRA-SVPWM, thanks to the combined effect of vector reordering and variable carrier frequency, the effective. This significantly higher frequency shifts more harmonics out of critical frequency bands, improving the output waveform (Figure 6).

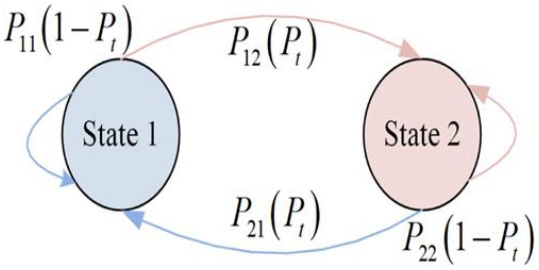

Figure 6: Diagram of state transition

Furthermore, from a signal-processing perspective, the modulation resembles a single-edge regularly sampled SVPWM, but with a variable-slope sampling plane. This plane is defined in a 3D space with axes representing time t, fundamental frequency ω0, and carrier frequency ωc. The plane shifts from a red one in the first half-cycle to a purple one in the second, due to the asymmetrical witching pattern. These shifting planes alter the timing of the PWM edges, thereby modifying the waveform's harmonic structure. The PWM voltage waveform can be decomposed into two parts: one defined before the plane shift, and one after, with their equations referenced at the bottom of the Original Figure. This technique is applied within a comprehensive IMC-PMSM (Integrated Modular Converter–Permanent Magnet Synchronous Motor) control system. The setup includes the PMSM as the load. The rectifier uses conventional SVPWM to process and sample the input voltages to control its switching behaviour. Meanwhile, the inverter employs the advanced MRA-SVPWM to enhance modulation efficiency. For motor control, a double closed-loop strategy with i_d = 0 and id = 0 is implemented for field-oriented control. The integration of MRA-SVPWM into this system results in improved switching behaviour, reduced harmonic content, and more efficient motor performance. A detailed control block diagram is presented in Fig. 13 to illustrate the implementation framework.

7. Comparative Analysis of Harmonic Distortion in Various PWM Algorithms

To validate the effectiveness of harmonic suppression, the phase current FFT results for various algorithms at r frequencies are analysed. These two frequencies are selected to represent typical conditions in industrial applications, where PMSM drives often operate at low speeds, especially in high-power systems. The comparison includes the conventional method, a hybrid of RCD and RSF methods, and the newly proposed method. In the analysis, the dashed lines in the FFT Figures represent the harmonic levels of the conventional SVPWM for reference, while solid lines indicate the performance. Conventional SVPWM exhibits high harmonic amplitudes, particularly at lower frequencies, where the effect is more pronounced. RCDPWM reduces first-order harmonic content but has a limited impact on higher-order harmonics. It also shifts harmonics towards lower frequencies, which could adversely affect motor control. On the other hand, RSFPWM suppresses second-order harmonics better but still falls short of fully mitigating harmonics across the spectrum.

To improve overall performance, a hybrid approach combining RCDPWM and RSFPWM is employed. This method achieves improved harmonic suppression compared to individual algorithms, but it still introduces some low-frequency harmonics due to the RCD component. The Markov chain RPWM enhances switching randomness, providing better suppression across both first- and second-order harmonic ranges. However, its performance is still constrained when it comes to consistent suppression beyond a certain threshold. The proposed MRA-SVPWM method outperforms all other strategies in reducing harmonic amplitudes near carrier frequency multiples. It achieves this by integrating Markov-based carrier frequency modulation with an optimised switching vector sequence to increase the effective switching frequency. This dual strategy results in significant suppression of high-frequency harmonics and avoids the drawbacks of low-frequency harmonic amplification. Acoustic noise analysis confirms that the proposed method effectively reduces motor noise, making it well-suited for applications that demand low-noise operation in industrial and transmission systems (Figure 7).

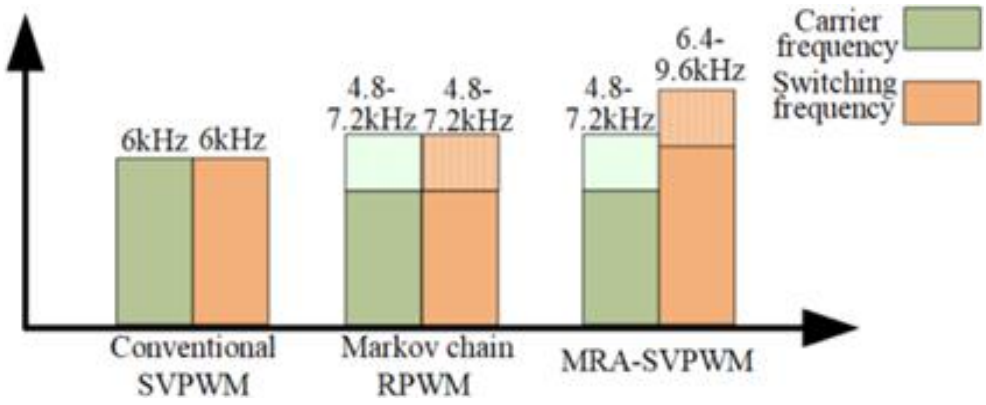

Figure 7: Frequency levels

8. Experiment Results

8.1. Harmonics Comparison of Different Algorithms

The simulation model represents a motor drive system controlled through (RPWM) techniques, integrated with a microcontroller unit, motor driver circuitry, and various protection mechanisms. It is designed to model the efficient and stable operation of a motor in applications that require precise speed control, rapid dynamic response, and high efficiency, such as industrial automation, robotics, and smart mobility systems. The system uses a combination of PWM switching, power electronics, and basic embedded control logic to simulate a real-world motor control environment.

8.2. System Overview

The simulation aims to model real-world behaviours, such as start-up dynamics, acceleration, load handling, and steady-state performance, under controlled switching patterns. Additionally, the model ensures safe operating conditions.

8.3. PWM Generation and Motor Driving

The PWM signals, the core element of this simulation, are generated with specific duty cycles corresponding to desired motor speeds. Voltage and thus faster motor rotation, while. The PWM generation module simulates the embedded microcontroller's timer and switching logic, converting user-defined speed inputs into accurate gate signals for the motor. These gate signals switch the motor driver’s transistors rapidly, delivering the necessary pulse-width-modulated voltage to the motor terminals. This allows the system to achieve fine-grained control over motor speed without introducing significant power losses.

8.4. Motor Model and Dynamic Behaviour

The motor itself is modelled as an electromechanical load with inertia, back EMF generation, and frictional losses. When the PWM-controlled voltage is applied, the acceleration depends on the applied voltage and the system's load conditions. Back EMF is inherently considered, influencing the current drawn from the driver as the motor speeds up. The dynamic behaviour—acceleration profiles, load torque impact, and steady-state stability—is closely monitored using real-time simulation scopes for speed and current.

8.5. Protection, Filtering, and Stability

To ensure operational safety and electromagnetic compatibility, the simulation includes basic filtering and protection features. A low-pass filter smoothens the motor voltage, reducing the high-frequency ripple caused by rapid PWM switching. Current-sensing blocks monitor motor current in real time; if current exceeds threshold levels (due to stall conditions or a sudden load increase), simulated protection logic can reduce the PWM duty cycle or temporarily shut off the driver to protect the system components.

8.6. Role of Control Logic and Switching Strategy

The control strategy implemented here is open-loop PWM, which can be extended to closed-loop control (e.g., speed feedback via PID controllers) if desired. The simulation also highlights the management of switching sequences (Figure 8).

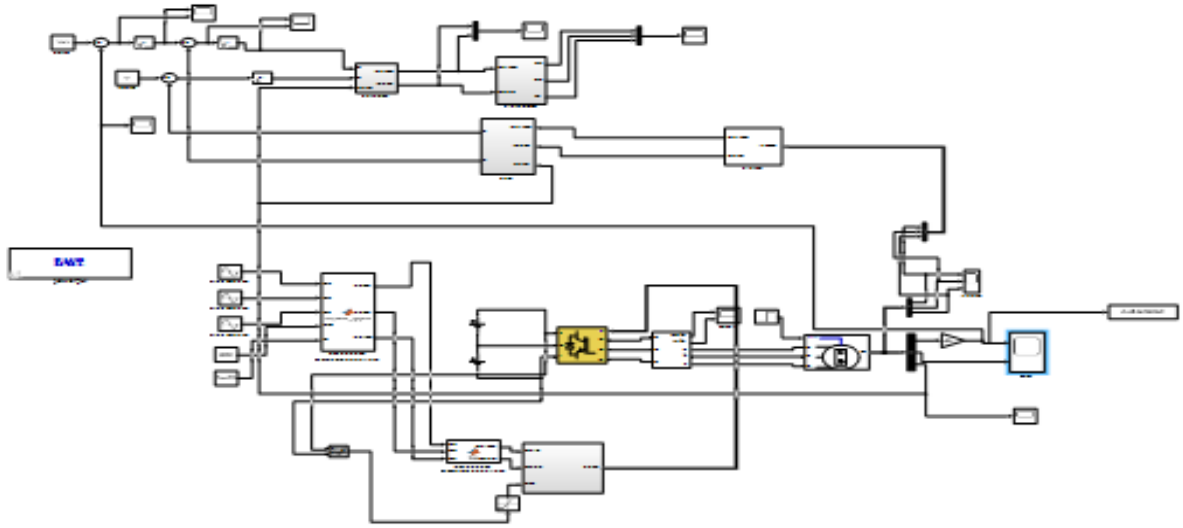

Figure 8: Simulation diagram

8.7. Uses of the Components

Toroidal inductors are also used in conjunction with these capacitors to filter out high-frequency noise, thus improving the overall power quality and protecting sensitive components from voltage fluctuations. To ensure a stable, smooth DC output, large filter capacitors are employed to reduce the ripple typically present after rectification. The acoustic vibration waveforms of the motor case and sole test points at 1 kHz and 6 kHz carrier frequencies were measured using a high-precision vibration sensor with conventional SVPWM and MRA-SVPWM. The red line and numbers show the amplitudes of harmonics at the lower integer multiples of the carrier frequency. The blue line and numbers show the amplitude and reduction of harmonics in the frequency spectrum above 10 kHz. The results show that the proposed algorithm can reduce motor noise by more than 10 dB (Figure 9).

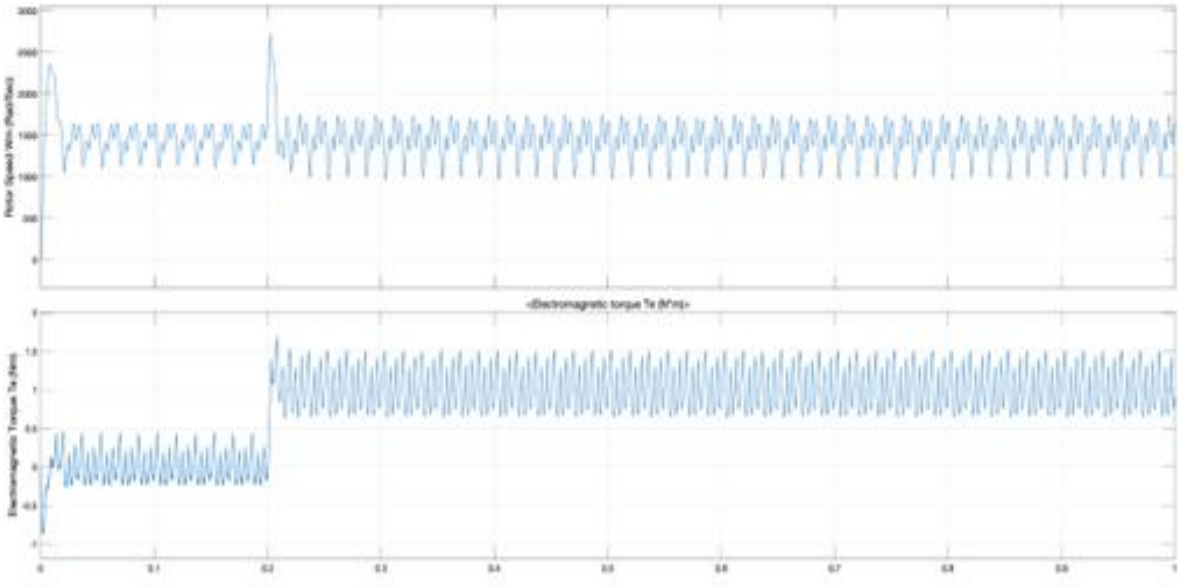

Figure 9: Torque and rotor speed output

This graph plots torque and rotor speed over time, both on the Y-axis. The smooth torque curve indicates stable electromagnetic performance, while the rotor speed curve shows a consistent rise and steady-state behaviour. The minimal oscillations and overshoot suggest that the RPPM technique has improved dynamic response and reduced ripple during load transitions (Figure 10).

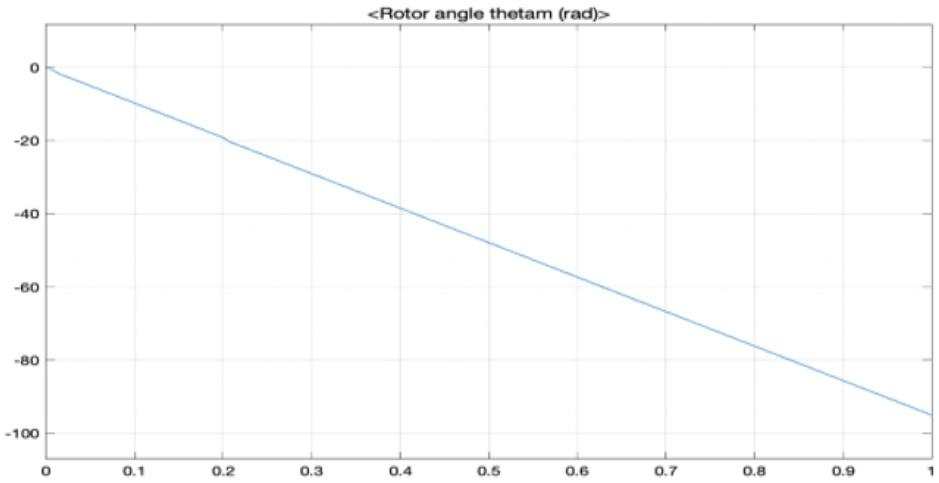

Figure 10: Rotor angle output

This graph represents rotor angle as a function of time or electrical cycles. The linear and progressive increase in rotor angle confirms a constant rotational velocity after an initial transient phase. This indicates effective speed regulation and synchronisation, which are further stabilised by the modulation scheme's noise-suppression characteristics (Figure 11).

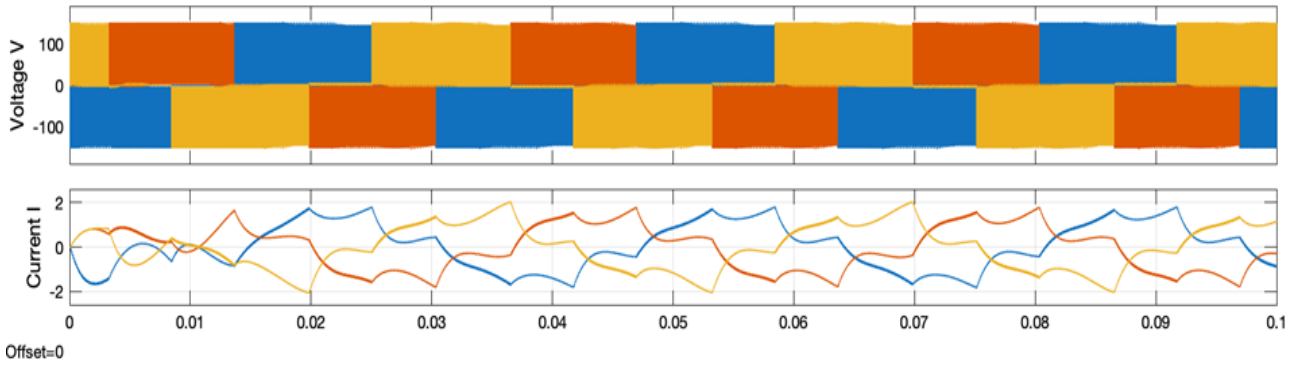

Figure 11: Three-phase inverter output

This graph shows the waveform of the three-phase system using MOSFET switches. The waveform exhibits random variations in the pulse pattern, a direct result of using Random Pulse Position Modulation (RPPM). The scattered harmonic energy distribution reduces peak EMI levels, effectively suppressing electrical noise. The clean transitions indicate good switching performance and low distortion (Figure 12).

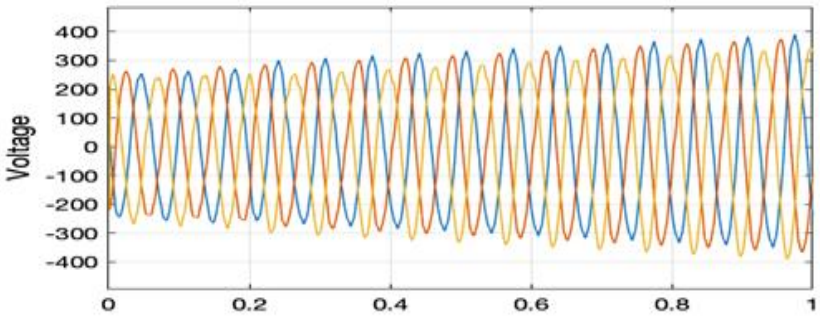

Figure 12: Clarke transformation output

This graph illustrates the transformed components of the motor current. The Clarke converts the currents into two orthogonal components. The smooth, sinusoidal-like waveform with minimal spikes reflects the modulation technique's effective suppression of high-frequency noise components. It confirms that RPPM improves current symmetry and reduces electromagnetic interference (Figure 13).

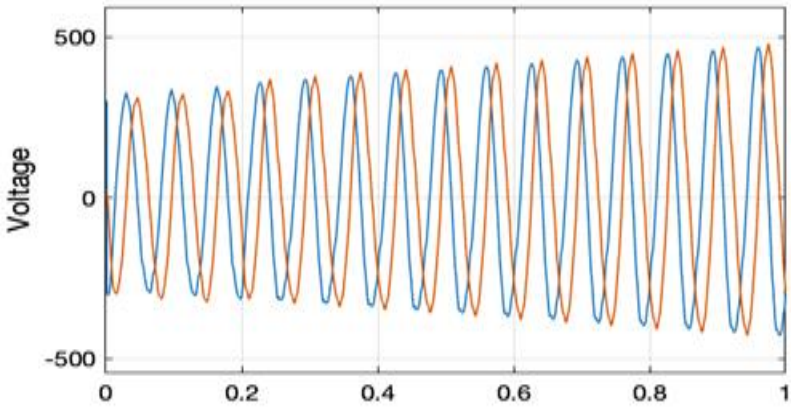

Figure 13: Park transformation output

This plot shows the d–q axis components derived from the Clarke outputs using the Park transformation. These components are used for vector control of the PMSM.

8.8. FFT Analysis Output

The waveform shows significant harmonic content at multiple frequencies beyond the fundamental 50 Hz, as seen in the bar graph. The Total Harmonic Distortion (THD) is 40.71%, which indicates a high level of harmonic interference. This level of distortion can lead to electromagnetic interference, reduced motor efficiency, and overheating, underscoring the need for an effective modulation strategy.

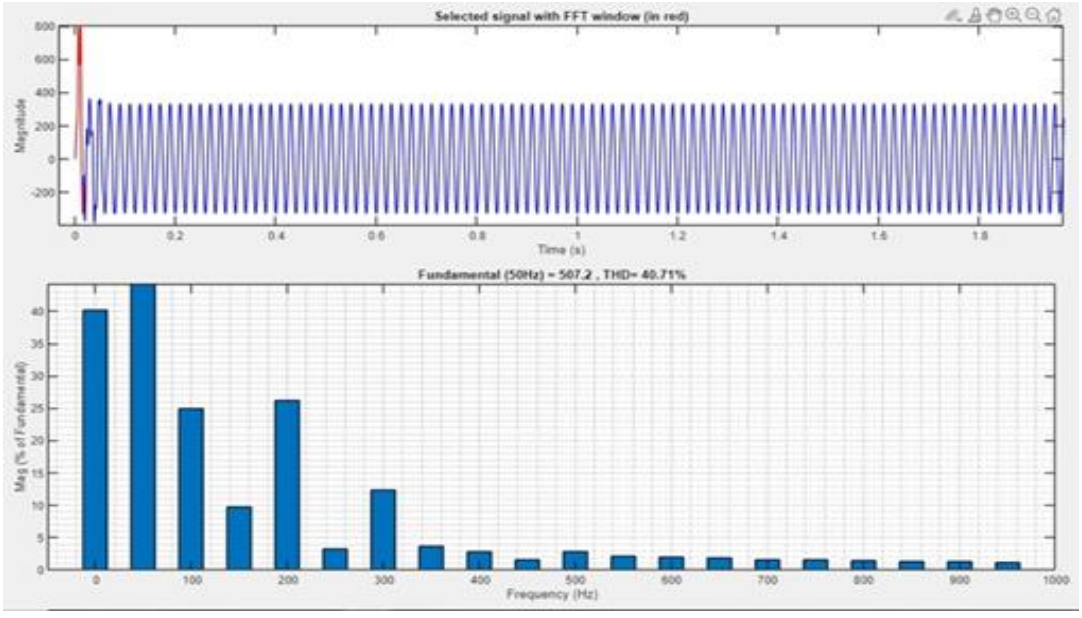

Figure 14: FFT in the starting window

Figure 14 shows the FFT result after applying Random Pulse Position Modulation. The harmonic content is drastically reduced across the spectrum, resulting in a much cleaner signal with fewer peaks beyond, now 0.57%, indicating a significant reduction in noise and harmonics (Figure 15).

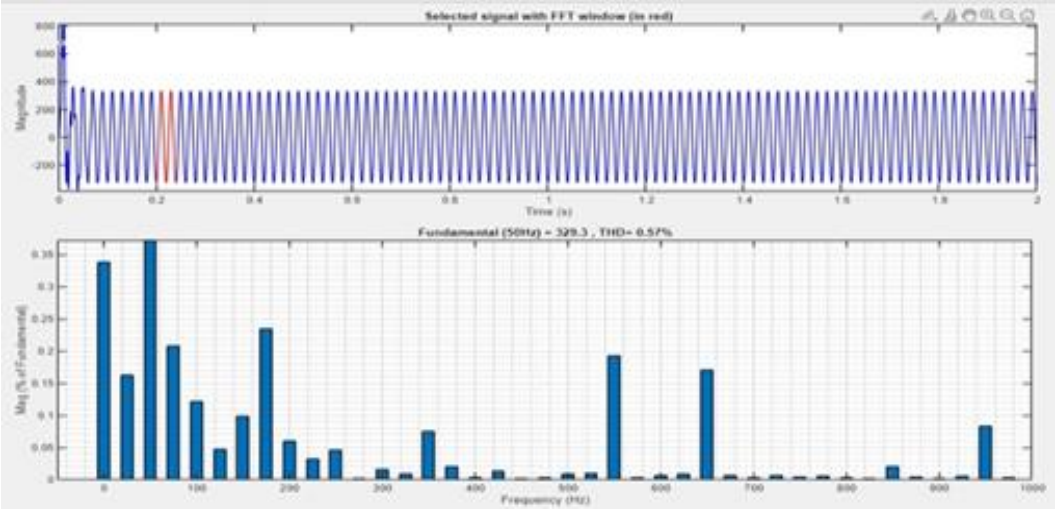

Figure 15: FFT in running window

This improvement validates the effectiveness of RPPM in minimising switching noise and enhancing the quality of the inverter output signal in PMSM drive systems.

8.9. Hardware Results

The AC power input cable supplies the necessary voltage, typically 220V at 50/60 Hz, to the system, acting as the primary source of energy for the entire setup. This AC voltage is fed into the bridge rectifier module mounted on the brown PCB, where it is converted into an unregulated DC voltage suitable for electronic operations. To ensure a stable, smooth DC output, large filter capacitors are employed to reduce the ripple typically present after rectification. Toroidal inductors are also used in conjunction with these capacitors to protect sensitive components from voltage fluctuations (Figure 16).

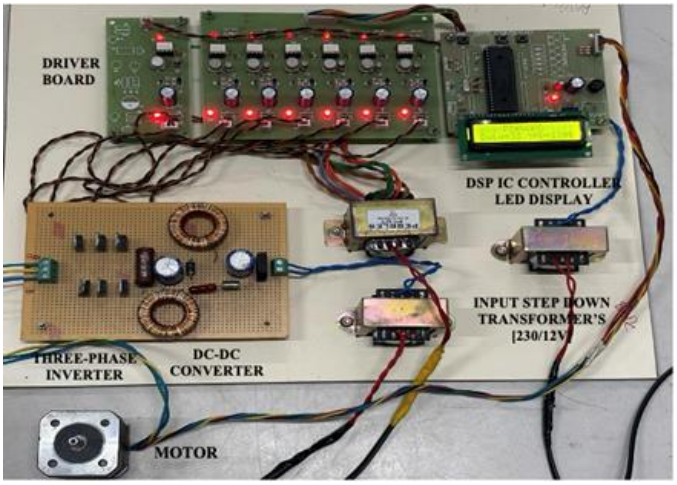

Figure 16: Hardware kit

Electromagnetic relays, visible as the metallic components labelled "Pebbles," function as electrically controlled switches that allow low-power control signals from the microcontroller to operate higher-power devices, such as motors and external loads. The stepper motor, connected to the driver circuits, provides precise rotational movement in discrete steps and accurate position control. The green PCB, which contains multiple LEDs and drive circuits, acts as an interface between the microcontroller. The microcontroller, located near the LCD board, serves as the system's brain, executing control algorithms, monitoring sensor inputs, and coordinating relay and motor driver operations. The LCD module displays key real-time parameters such as motor direction, step count, and system status, providing important feedback to the user. Finally, a network of signal and power wiring interconnects all modules, ensuring reliable communication and efficient power distribution across the system, thus enabling coordinated and safe functioning of the overall hardware setup (Figure 17).

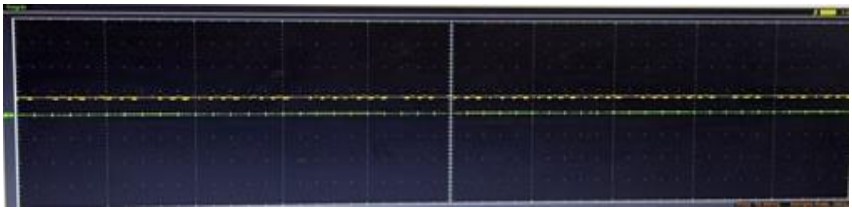

Figure 17: Transformer input

This waveform shows the supply input to the step-down transformer, from which the DSP IC Controller receives a constant 5V pulse (Figure 18).

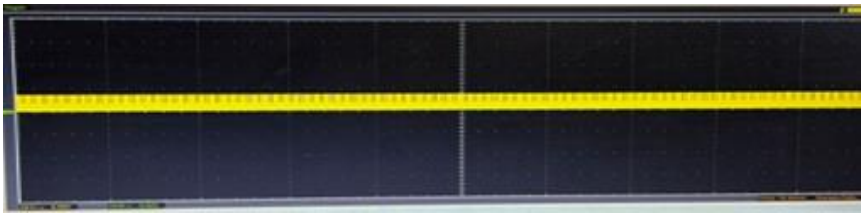

Figure 18: Microcontroller signal

Researchers can see that the IC has processed the signal as desired and sent it to the seven-leg driver board as a 5V pulse (Figure 19).

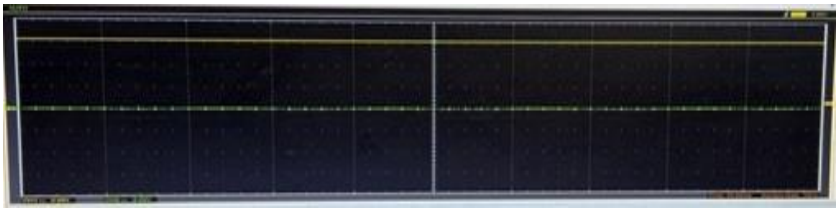

Figure 19: Driver board input

This shows the amplified input from the second transformer to the driver board, with seven taps providing an output of 15V (Figure 20).

Figure 20: Driver board output

Researchers can see that the driver board receives input from the controller and transformer switches, amplifies the 5V signal to 9V, and provides it to the inverter (Figure 21).

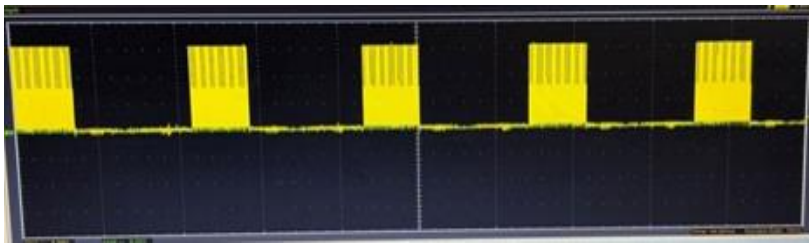

Figure 21: Modulated pulse output

As the Duty cycle is increased through the button, the speed naturally increases, and the pulse width (duration) consequently decreases, as depicted.

9. Conclusion

The suggested control framework demonstrated steady speed regulation, precise torque control, and smooth dynamic response across a wide range of load conditions, thanks to careful system design, modelling, and simulation. The system was able to maintain the necessary operating parameters stable under both transient and steady-state conditions. This meant little overshoot, a quick settling period, and fewer speed changes. These traits show how effective the control technique is at handling changes and external factors. The hardware implementation confirmed that the suggested method worked well. The system got excellent computational efficiency and consistent real-time performance by combining modern motor control techniques with a microcontroller-based platform. Careful use of pulse-width modulation (PWM) techniques improved switching behaviour, resulting in lower switching losses and less thermal stress on power electronic components. This improved the system's performance and longevity. Also, the control design ensured torque was well controlled by quickly responding to load variations, improving the drive's overall performance. The hardware and software worked together perfectly, enabling smooth transitions between operating states without instability or oscillations. Experimental observations confirmed that the system consistently delivered dependable performance while maintaining energy efficiency, even under challenging operational conditions. The microcontroller-based control system is small and versatile, which makes it easy to scale up and adapt to different uses. The proposed solution is well-suited for real-world use because it simplifies the system and is inexpensive to implement. The system's ability to consistently perform well in real-world situations also demonstrates that it can be used in modern electric motor systems. Overall, the results show that microcontroller-based motor control schemes achieve high efficiency, dependable operation, and improved dynamic performance. The suggested solution is ideal for real-world applications, including electric cars, robotic platforms, and factory automation, where accuracy, efficiency, and reliability are key performance goals.

Acknowledgement: The authors gratefully acknowledge the academic support and institutional resources provided by SRM Institute of Science and Technology, University of Dubrovnik, Urgench State University, and Dhaanish Ahmed College of Engineering, which contributed to this collaborative work.

Data Availability Statement: The data supporting the findings of this study are included in this study, with additional datasets available from the corresponding authors upon reasonable request.

Funding Statement: This research was jointly carried out by the authors without receiving any external funding or financial support.

Conflicts of Interest Statement: The authors collectively declare that there are no conflicts of interest related to this manuscript. All sources of information have been appropriately cited and acknowledged.

Ethics and Consent Statement: Ethical approval was obtained before conducting the study, and informed consent was obtained from all participating organisations and individuals, where applicable. All authors confirm that the research complied with relevant ethical standards and guidelines.

References

1. J. W. Kolar, T. Friedli, J. Rodriguez, and P. W. Wheeler, “Review of three-phase PWM AC–AC converter topologies,” *IEEE Transactions on Industrial Electronics*, vol. 58, no. 11, pp. 4988–5006, 2011.
2. M. Aguirre, S. Kouro, C. A. Rojas, and S. Vazquez, “Enhanced switching frequency control in FCS-MPC for power converters,” *IEEE Transactions on Industrial Electronics*, vol. 68, no. 3, pp. 2470–2479, 2020.
3. W. Song, Y. Yang, W. Qin, and P. Wheeler, “Switching state selection for model predictive control based on genetic algorithm solution in an indirect matrix converter,” *IEEE Transactions on Transportation Electrification*, vol. 8, no. 4, pp. 4496–4508, 2022.
4. Y. Zhang, Z. Yin, X. Cao, Y. Zhang, and J. Liu, “A novel SPMSM sensorless drive using discrete-time synchronous-frequency adaptive observer under low frequency ratio,” *IEEE Transactions on Power Electronics*, vol. 37, no. 9, pp. 11045–11057, 2022.
5. Y. Ge, L. Yang, and X. Ma, “A harmonic compensation method for SPMSM sensorless control based on the orthogonal master-slave adaptive notch filter,” *IEEE Transactions on Power Electronics*, vol. 36, no. 10, pp. 11701–11711, 2021.

6. S. V. Nair, P. Harikrishnan, and K. Hatua, “Six-step operation of a symmetric dual three-phase PMSM with minimal circulating currents for extended speed range in electric vehicles,” *IEEE Transactions on Industrial Electronics*, vol. 69, no. 8, pp. 7651–7662, 2021.
7. A. Ruiz-Gonzalez, F. Vargas-Merino, J. R. Heredia-Larrubia, M. J. Meco-Gutierrez, and F. Perez-Hidalgo, “Application of slope PWM strategies to reduce acoustic noise radiated by inverter-fed induction motors,” *IEEE Transactions on Industrial Electronics*, vol. 60, no. 7, pp. 2555–2563, 2013.
8. M. Farasat, A. Arabali, and A. M. Trzynadlowski, “Flexible-voltage DC-bus operation for reduction of switching losses in all-electric ship power systems,” *IEEE Transactions on Power Electronics*, vol. 29, no. 11, pp. 6151–6161, 2014.
9. Y. Huang, Y. Xu, W. Zhang, and J. Zou, “Hybrid RPWM technique based on modified SVPWM to reduce the PWM acoustic noise,” *IEEE Transactions on Power Electronics*, vol. 34, no. 6, pp. 5667–5674, 2018.
10. Y. Xu, W. Zhang, Y. Huang, and J. Zou, “Multisector three-phase PMSM drive system with low-frequency and high-frequency PWM noise,” *IEEE J. Emerg. Sel. Topics Power Electron.*, vol. 10, no. 2, pp. 1639–1648, 2022.
11. S. Y. Oh, Y. G. Jung, S. H. Yang, and Y. C. Lim, “Harmonic-spectrum spreading effects of two-phase random centered distribution PWM (DZRCD) scheme with dual zero vectors,” *IEEE Trans. Ind. Electron.*, vol. 56, no. 8, pp. 3013–3020, 2009.
12. K. Lee, G. Shen, W. Yao, and Z. Lu, “Performance characterization of random pulse width modulation algorithms in industrial and commercial adjustable-speed drives,” *IEEE Trans. Ind. Appl.*, vol. 53, no. 2, pp. 1078–1087, 2017.
13. P. Madasamy, R. Verma, C. Bharatiraja, B. P. J. Glady, T. Srihari, J. L. Munda, and L. Mihet-Popa, “Hybrid multicarrier random space vector PWM for the mitigation of acoustic noise,” *Electronics*, vol. 10, no. 12, p. 1483, 2021.
14. P. Zhang, S.Wang, and Y. Li, “Performance and analysis of N-state random pulse position SVPWM with constant sampling frequency,” *IEEE Trans. Power Electron.*, vol. 37, no. 11, pp. 13606–13625, 2022.
15. A. Peyghambari, A. Dastfan, and A. Ahmadyfard, “Selective voltage noise cancellation in three-phase inverter using random SVPWM,” *IEEE Trans. Power Electron.*, vol. 31, no. 6, pp. 4604–4610, 2024.